

# A Mammalian Protein Homologous to Fructosamine-3-Kinase Is a Ketosamine-3-Kinase Acting on Psicosamines and Ribulosamines but not on Fructosamines

François Collard,<sup>1</sup> Ghislain Delpierre,<sup>1</sup> Vincent Stroobant,<sup>2</sup> Gert Matthijs,<sup>3</sup> and Emile Van Schaftingen<sup>1</sup>

Fructosamine-3-kinase (FN3K) is an enzyme that appears to be responsible for the removal of fructosamines from proteins. In this study, we report the sequence of human and mouse cDNAs encoding proteins sharing 65% sequence identity with FN3K. The genes encoding FN3K and FN3K-related protein (FN3K-RP) are present next to each other on human chromosome 17q25, and they both have a similar 6-exon structure. Northern blots of mouse tissues RNAs indicate a high level of expression of both genes in bone marrow, brain, kidneys, and spleen. Human FN3K-RP was transfected in human embryonic kidney (HEK) cells, and the expressed protein was partially purified by chromatography on Blue Sepharose. Unlike FN3K, FN3K-RP did not phosphorylate fructoselysine, 1-deoxy-1-morpholino-fructose, or lysozyme glycosylated with glucose. In a more systematic screening for potential substrates for FN3K-RP, we found, however, that both enzymes phosphorylated ketosamines with a D-configuration in C3 (psicoselysine, 1-deoxy-1-morpholino-psicose, 1-deoxy-1-morpholino-ribulose, lysozyme glycosylated with allose—the C3 epimer of glucose, or with ribose). Tandem mass spectrometry and nuclear magnetic resonance analysis of the product of phosphorylation of 1-deoxy-1-morpholino-psicose by FN3K-RP indicated that this enzyme phosphorylates the third carbon of the sugar moiety. These results indicate that FN3K-RP is a ketosamine-3-kinase (ketosamine-3-kinase 2). This enzyme presumably plays a role in freeing proteins from ribulosamines or psicosamines, which might arise in a several step process, from the reaction of amines with glucose and/or glycolytic intermediates. This role is shared by fructosamine-3-kinase (ketosamine-3-kinase 1), which has, in addition, the unique capacity to phosphorylate fructosamines. *Diabetes* 52:2888–2895, 2003

From the <sup>1</sup>Laboratory of Physiological Chemistry, ICP, and Université Catholique de Louvain, Brussels, Belgium; the <sup>2</sup>Brussels Branch of the Ludwig Institute, Brussels, Belgium; and the <sup>3</sup>Center for Human Genetics, University of Leuven, Leuven, Belgium.

Address correspondence and reprint requests to E. Van Schaftingen, Avenue Hippocrate 75, B-1200, Brussels, Belgium. E-mail: vanschaftingen@bcm.ucl.ac.be.

Received for publication 10 March 2003 and accepted in revised form 15 September 2003.

COSY, correlation spectra; EST, expressed sequence tag; FISH, fluorescence in-situ hybridization; FN3K, fructosamine-3-kinase; FN3K-RP, FN3K-related protein; HEK, human embryonic kidney; HMBC, heteronuclear multiple bond connectivity; NMR, nuclear magnetic resonance; RACE, rapid amplification of complementary DNA ends.

© 2003 by the American Diabetes Association.

Primary amines of proteins and other compounds spontaneously react with carbohydrates that possess a free carbonyl group to produce Schiff bases. These slowly rearrange to form Amadori or Heyns products, depending on whether the reacting sugar was an aldose or a ketose (1–4). This process, known as nonenzymatic glycation, is best known for glucose, leading then to the production of fructosamines. Similar reactions occur with other sugars (mannose, galactose, fructose, and pentoses) (5) and phosphorylated sugar derivatives (6–8). In fact, glucose is intrinsically one of the least reactive sugars in this respect because it is well stabilized in its hemiacetalic form (5).

Formation of fructosamines has attracted much attention in the context of diabetes. This is because the glycation rate is first order with respect to glucose concentration. Serum fructosamines and glycosylated hemoglobin are therefore assayed to assess the blood glucose concentration in the preceding weeks or months (9–11). Furthermore, fructosamines are thought to participate in the pathogenesis of long-term diabetes complications by acting either as such (12) or after conversion to advanced glycation end products (13–15).

The sequence of a mammalian protein that catalyzes the phosphorylation of low-molecular weight and protein-bound intracellular fructosamines on the third carbon of their deoxyfructose moiety has recently been reported (16,17). Because fructosamine 3-phosphate residues are unstable (17), fructosamine-3-kinase (FN3K) appears to cause the removal of fructosamine residues from proteins. Accordingly, 1-deoxy-1-morpholino-fructose, a (substrate and) competitive inhibitor of FN3K, caused a twofold increase in the accumulation of glycosylated hemoglobin in erythrocytes incubated with 200 mmol/l glucose (18).

While cloning the cDNA encoding FN3K, we noted the existence of human and mouse cDNAs encoding a related protein. In this study, we report the sequence of this FN3K-related protein (FN3K-RP) and the identification of its biochemical function.

## RESEARCH DESIGN AND METHODS

**Preparation of ketosamines.** Psicoselysine was synthesized from allose and t-BOC-lysine and purified as previously described for fructoselysine (18,19). 1-Deoxy-1-morpholino-psicose, 1-deoxy-1-morpholino-ribulose, and 1-deoxy-

1-morpholino-xylose were synthesized from morpholine and allose, ribose, or xylose, respectively (20). The incubation time after the addition of ethanol was reduced to 15 min in the last two cases. The products were purified on AG50WX4 (H<sup>+</sup> form) columns from which they were eluted with 500 mmol/l NaCl. They were desalted by gel filtration on Biogel P2 and quantified by measuring the reducing power (21), using 1-deoxy-1-morpholino-fructose as a standard. Mass spectrometry analysis indicated that the products had the expected m/z ratio. Their purity was checked by paper chromatography on 3 MM paper in two different solvents (ethylacetate/pyridine/water: 12/5/4 and ethylacetate/water/acetic acid/formic acid: 18/4/3/1) and estimated to >95% for psicoselysine, 1-deoxy-1-morpholino-psicose, and 1-deoxy-1-morpholino-xylose, and to ~70% for 1-deoxy-1-morpholino-ribose. Using this method, we could ascertain that psicoselysine and 1-deoxy-1-morpholino-psicose were not contaminated with their C3 epimers, which had distinct Rfs. 1-Deoxy-1-morpholinoribulose appeared to be contaminated with ~20% 1-deoxy-1-morpholinoxylose.

[<sup>14</sup>C]1-deoxy-1-morpholino-ribose was synthesized by incubating 12.5 μCi [1-<sup>14</sup>C]ribose (American Radiochemical) with 30 μl morpholine at 75°C; 8 μl acetic acid and 40 μl ethanol were added after 30 and 40 min, respectively, and the incubation pursued for 15 min. Further purification on the cation exchanger (see above) resulted in a product that could be phosphorylated by FN3K or FN3K-RP to an extent of ~50%. A more pure radiolabeled compound was obtained by purifying this product of phosphorylation with FN3K (obtained after a 40-min incubation at 30°C in the presence of 1.2 mU/ml FN3K, 5 mmol/l ATP-Mg, 25 mmol/l Tris, pH 7.8, 1 mmol/l EGTA, 1 mmol/l MgCl<sub>2</sub>, in a final volume of 10 ml) on an anion exchanger (AG1X8). The purified phosphorylation product was dephosphorylated with alkaline phosphatase, which was denatured with perchloric acid. More than 90% of the radioactive product could then be phosphorylated with FN3K or FN3K-RP.

For the synthesis of glycosylated lysozyme, a solution containing 60 mg/ml hen egg lysozyme, 25 mmol/l HEPES, pH 7.1, and 1 mol/l of the indicated aldoses was filtered on a 0.22-μm membrane and incubated at 37°C for 20 days (allose and glucose) or 3 days (ribose). Glycosylated lysozyme was purified by gel filtration on a Biogel P2 column equilibrated with water. The degree of glycosylation, estimated by nano-electrospray mass spectrometry, was 1.35 mol/mol for glucose, 3.35 for allose, and 4 for ribose, which is consistent with the higher reactivity of allose, and most particularly of ribose, as compared with glucose (5).

**Sequencing and preparation of expression vectors.** Human expressed sequence tag (EST) clones AI202129 and AI244490 were ordered from the U.K. Human Genome Mapping Project Resource Centre and sequenced (16). Rapid amplification of complementary DNA ends (RACE) (5' and 3') was carried out on mouse brain cDNA using the corresponding kits from Gibco BRL (Gaithersburg, MD). The amplification products were subcloned in pBluescript and sequenced. For the preparation of the bacterial expression vectors, a 5' primer containing the putative ATG codon in an *NdeI* site and a 3' primer containing the putative stop codon flanked by a *BglIII* (human) or *EcoRV* (mouse) site were used to amplify human kidney or mouse brain cDNA with *Pwo* polymerase. The amplification products were subcloned in pBluescript, checked by sequencing, and inserted between the *NdeI* and *BamHI* sites of pET3a. For the preparation of the eukaryotic expression vector, the open-reading frame of human FN3K (16) and FN3K-RP, flanked with a perfect Kozak (22) consensus sequence (CCACCATGC), were PCR amplified with *Pwo* polymerase using the appropriate plasmids as templates and inserted between the *EcoRI* and *BamHI* sites (for FN3K) or *EcoRI* and *XbaI* sites (for FN3K-RP) of pCMV5.

**Overexpression and purification of proteins.** HEK-293 cells were cultured under 5% CO<sub>2</sub> at 37°C in Dulbecco's minimal essential medium containing 10% (vol/vol) FCS in 10-cm diameter Sarstedt dishes coated with poly-L-lysine. They were transfected using a modified calcium phosphate procedure (23) with 7.5 μg pCMV5 DNA and incubated overnight at 37°C under 3% CO<sub>2</sub>. The medium was replaced with fresh Dulbecco's minimal essential medium containing 10% (vol/vol) FCS, and the incubation was pursued at 37°C in the presence of 5% CO<sub>2</sub>. Cells were harvested after 48 h in 0.75 ml of a buffer containing 25 mmol/l HEPES, pH 7.1, 5 mg/l leupeptin, 5 mg/l antipain, and 0.5 mmol/l phenylmethylsulfonyl fluoride. After three cycles of freezing and thawing, the cell lysates were centrifuged for 30 min at 20,000g and 4°C.

The supernatant obtained from ~20 dishes (~175 mg protein) was diluted with two volumes of buffer A (25 mmol/l HEPES, pH 7.1, 5 mg/l leupeptin, and 5 mg/l antipain) and loaded onto a 5-ml Blue Sepharose column at 4°C. The column was washed with 5 ml of buffer A and then with increasing NaCl concentration in buffer A. Protein was measured according to Bradford (24) with bovine γ-globulin as a standard.

For the Western blots, proteins were separated in 10% SDS-polyacrylamide gels, transferred onto nitrocellulose membranes, and probed with rabbit polyclonal antibodies directed against recombinant human FN3K at a 1/1,000

dilution and then with horseradish peroxidase-conjugated anti-rabbit IgG (Sigma) at a 1/2,000 dilution. Immunocomplexes were visualized with the enhanced chemiluminescence reaction (Amersham Pharmacia Biotech). The amount of FN3K-RP and FN3K was estimated by comparing the intensity of bands corresponding to these proteins in Coomassie Blue-stained SDS-PAGE gels with those of protein standards.

**RNA extraction and Northern blotting.** Total RNA was isolated from tissues from male 30-g NMR mice (from Charles River) using the Ambion RNA-WIZ kit. Northern blots were performed (25) on 25 μg total RNA for all tissues, except for lenses, for which only ~0.5 μg could be loaded. The probes used were the PCR-amplification products of the open-reading frames of mouse FN3K and FN3K-RP labeled with [α-<sup>32</sup>P] dCTP by random priming.

**Measurement of enzymatic activity.** Phosphorylation of 1-deoxy-1-morpholino-fructose, 1-deoxy-1-morpholino-psicose, and psicoselysine was assayed at 30°C in a mixture containing 25 mmol/l Tris, pH 7.8, 1 mmol/l EGTA, 1 mmol/l MgCl<sub>2</sub>, 1 mmol/l dithiothreitol, 50 μmol/l ATP-Mg, and 500,000 cpm [γ-<sup>32</sup>P]ATP in a final volume of 60 μl. The reaction was stopped by adding 90 μl ice-cold 10% (w/vol) perchloric acid. After neutralization with K<sub>2</sub>CO<sub>3</sub>, the supernatants were diluted to 1 ml with 20 mmol/l MES, pH 6, and loaded onto anion-exchange columns (AG1X8, Cl<sup>-</sup> form, 1 ml). These were then washed with five volumes of 20 mmol/l MES, pH 6, to elute the phosphorylated Amadori compound, the unreacted [γ-<sup>32</sup>P]ATP remaining bound to the column. The eluate was mixed with 15 ml OptimaGold (Packard) scintillation fluid and counted for radioactivity. Phosphorylation of glycosylated lysozyme was assayed by incorporation of <sup>32</sup>P from [γ-<sup>32</sup>P]ATP (16) in a mixture containing 25 mmol Tris, pH 7.8, 1 mmol/l EGTA, 1 mmol/l MgCl<sub>2</sub>, 1 mmol/l dithiothreitol, 2.1 mg/ml glycosylated hen egg lysozyme, and 100 μmol/l ATP-Mg. Phosphorylation of 1-deoxy-1-morpholino-ribose was measured using [<sup>14</sup>C]1-deoxy-1-morpholino-ribose, as previously described for [<sup>14</sup>C]1-deoxy-1-morpholino-fructose (16).

**Preparation of phosphorylated 1-deoxy-1-morpholino-psicose for nuclear magnetic resonance and mass spectrometry analysis.** 1-Deoxy-1-morpholino-psicose (25 μmol) was incubated for 18 h at 30°C in a final volume of 10 ml in the presence of 25 mmol/l Tris, pH 7.8, 1 mmol/l EGTA, 1 mmol/l dithiothreitol, 2 mmol/l ATP-Mg, 0.5 mg/ml BSA, and 1.1 mU of partially purified human recombinant FN3K-RP. The reaction medium was mixed with 2 ml ice-cold 70% (vol/vol) HClO<sub>4</sub> and centrifuged for 20 min at 16,000g and 4°C. The supernatant was brought to neutral pH by mixing with 50 ml of a *tris*-N-octylamine/chloroform (1/3.6) mixture. The aqueous phase was diluted in water to a final volume of 45 ml and applied onto a 25-cm<sup>3</sup> AG1X8 (Cl<sup>-</sup>) column, which was washed with 70 ml water to elute unreacted 1-deoxy-1-morpholino-psicose, and a linear NaCl gradient (2 × 125 ml; 0–0.5 mol/l NaCl) was applied to elute 1-deoxy-1-morpholino-psicose-phosphate. Fractions of 3 ml were collected, and the reducing power was measured (21). Fractions containing 1-deoxy-1-morpholino-psicose-phosphate were pooled and concentrated under vacuum to 2 ml and applied on a BiogelP2 column equilibrated in water to remove salts.

Mass spectrometry analysis was carried out as previously described (26). For the nuclear magnetic resonance (NMR) analysis, the preparation of 1-deoxy-1-morpholino-psicose-phosphate was evaporated to dryness, and the residue was dissolved in deuterated water. The pH of the final solution was 6.0. All NMR spectra were acquired on a Bruker DRX500 spectrometer at 30°C using a 5-mm probe head for inversion detection. Standard Bruker pulse programs were used to obtain one-dimensional phosphorus spectra (with and without proton decoupling), proton spectra (with and without phosphorus decoupling), <sup>1</sup>H-<sup>1</sup>H correlation spectra (COSY), and <sup>1</sup>H-<sup>31</sup>P-spectra (heteronuclear multiple bond connectivity [HMBC]). A delay of 50 ms was used for evolution of <sup>3</sup>J<sub>PH</sub> constants. <sup>31</sup>P chemical shifts were referenced to external 85% H<sub>3</sub>PO<sub>4</sub> and proton chemical shifts and to 3-(trimethylsilyl)propanesulfonic acid (sodium salt).

## RESULTS

**Identification of cDNA encoding FN3K-RP.** Basic local alignment search tool searches with the sequence of FN3K allowed us to identify several human ESTs and one mouse EST that encoded proteins homologous to FN3K. Human cDNAs (clones 1865439 and 1860099, corresponding to sequences AI244490 and AI202129) were ordered and completely sequenced to establish the primary structure of FN3K-RP. Both encoded the same 309 residue protein (identical to hypothetical protein FLJ12171, accession no. AAH07611) with a predicted mass of 34,412 Da and both had a 5' untranslated region of 17 nucleotides. They

FN3K <sub>HS</sub>	<b>MEQLLRAELRTATLRAFGGPGAGCISEGRAYDTDAGPFVFKVNR</b>	45
FN3K <sub>Mm</sub>	<b>MEQLLRAQLHTTTLRAFGSGGGCISEGYAYYDSDGPFVFKVNR</b>	45
FN3K-RP <sub>HS</sub>	<b>MEELLRLRELCSSVRAATGHSGGCISQGRSYDTDQGRVFKVNP</b>	45
FN3K-RP <sub>Mm</sub>	<b>METLLKRELGCSSVKAATGHSGGCISQGSYDTDKGRVFKVNSK</b>	45
FN3K <sub>HS</sub>	<b>TQARQMFEGEVAASLEALRSTGLVVRVPRPMKVIDLPGGGA</b>	90
FN3K <sub>Mm</sub>	<b>TQARQMFEGEMASLEALRNTGLVVRVPMKVIDLPGGGAVFVMEH</b>	90
FN3K-RP <sub>HS</sub>	<b>AEARRMFEGEMASLTALIKTNTVKVVKPKIKVLDAPGGGSVLVMEH</b>	90
FN3K-RP <sub>Mm</sub>	<b>AEARRMFEGEMASLTALIKTGTVKVVKPKIKVVDAPGGGSMLVMEH</b>	90
FN3K <sub>HS</sub>	<b>LKMKSLSQASKLGEQMDLHLYNQKLRKREKKEENTVGRRGE</b>	135
FN3K <sub>Mm</sub>	<b>LKMKSLSQASKLGEQMDLHLYNQKLRKREKSKTRONTVCGGAE</b>	135
FN3K-RP <sub>HS</sub>	<b>MDMRHLSSHAAKLGAQLADLHLDNKLKLGEMRLKEAGTVGRGGQE</b>	135
FN3K-RP <sub>Mm</sub>	<b>LDMRYLSSHATKLGTLADLHLENKRLGERLLKEAGTVGKGEQA</b>	135
FN3K <sub>HS</sub>	<b>EPQYVDKFGFHTVTCGGFIPQVNEWQDDWPTFFARHRLQAQLDLI</b>	180
FN3K <sub>Mm</sub>	<b>EPQGVTKFGFHTVTCGGFIPQVNEWQDDWPTFFRHRRLQAQLDLI</b>	180
FN3K-RP <sub>HS</sub>	<b>ERPFVAREFGFDVVTCCGYLPQVNDWQEDWVVFYARQRIQPQMDMV</b>	180
FN3K-RP <sub>Mm</sub>	<b>ERQYVDQFGFDVVTCCGYLPQVNDWQKNWVVFYARQRIQPQMDMV</b>	180
FN3K <sub>HS</sub>	<b>EKDYADREARELWSRLQVKIPDLFCGLEIVPALLHGDWLSGNVAE</b>	225
FN3K <sub>Mm</sub>	<b>EKDYADRETQELWSRLQVKIPDLFAGIEIVPALLHGDWLSGNVAE</b>	225
FN3K-RP <sub>HS</sub>	<b>ERESGDREALQLWSALQLKIPDLFRDLEIIPALLHGDWLSGNVAE</b>	225
FN3K-RP <sub>Mm</sub>	<b>ERKSGDREALLWSALQLKIPDLFRDLEIIPALLHGDWLSGNVAE</b>	225
FN3K <sub>HS</sub>	<b>DDVGPITIDPASFYGHSEFELAIAMFGGFPRSFYAYHRKIPKA</b>	270
FN3K <sub>Mm</sub>	<b>DDQGFVIYDPASFYGHSEFELAIAMFGGFPRSFYAYHRKIPKA</b>	270
FN3K-RP <sub>HS</sub>	<b>DSSGPIIDPASFYGHSEYELAIAMFGGFSSSFYSAYHGKIPKA</b>	270
FN3K-RP <sub>Mm</sub>	<b>DSSGPIIDPASFYGHSEYELAIAMFGGFSSSFYSAYHSKIPKT</b>	270
FN3K <sub>HS</sub>	<b>PGFDQRLLYQLFNYLNHNHFGREYRSPSLGTMRRLLK</b>	309
FN3K <sub>Mm</sub>	<b>PGFDKRLLYQLFNYLNHNHFGREYRSPSLGVMRKLRL</b>	309
FN3K-RP <sub>HS</sub>	<b>PGFEKRLQLYQLFHYLNHNHFGSGYRGSLSLIMRNLVK</b>	309
FN3K-RP <sub>Mm</sub>	<b>PGFEKRLQLYQLFHYLNHNHFGSGYRGSLSLIMRNLVK</b>	309

FIG. 1. Alignment of the sequences of mouse and human FN3K-RPs with those of human and mouse FN3Ks. Residues that are conserved in the four sequences are in bold type.

differed from each other through their 3' untranslated region, of 812 and 735 bp, respectively, and by two single nucleotide changes at positions 1433 and 1555.

The mouse cDNA sequence encoding FN3K-RP was established by 5' and 3' RACE experiments starting from EST sequence AI647859, which contains nucleotides 445–646 of the final cDNA sequence. The sequence that we obtained contained 48 bp of the 5' untranslated region and 78 bp of the 3' untranslated region (whose length is ~2 kb, see below). It encoded a protein identical to hypothetical protein XP-137924, which in the meantime had appeared in databanks.

The predicted human and mouse FN3K-RPs have the same length (309 amino acids) as human and mouse FN3Ks (Fig. 1). They share 88% sequence identity with each other and 64% sequence identity with human and mouse FN3Ks. Like FN3Ks, their second amino acid is a glutamate, which suggests that their NH<sub>2</sub>-terminal residue is an acetylated methionine (27), as is the case for FN3K (16). They are homologous to bacterial proteins of unknown function, with which they share 25–35% sequence identity (not shown). Like FN3K (16), FN3K-RP comprises an HGDxxxxN motif also found in aminoglycoside kinases.

**Gene structure and chromosomal localization of FN3K and FN3K-RP.** Basic local alignment search tool searches with the human genome sequences indicate that FN3K-RP is located in the telomeric region of the long arm of chromosome 17, next to the gene encoding FN3K (not shown). Both genes are separated by ~8.5 kb and have the same orientation, the gene encoding FN3K-RP being 5' with respect to the FN3K gene. They both have the same 6-exon structure, with the initiator ATG in exon 1 and the stop codon in exon 6. Their intron-exon junctions are in homologous position, and they both comprise a large fourth intron (7.5 kb in FN3K; 3.5 kb in FN3K-RP).

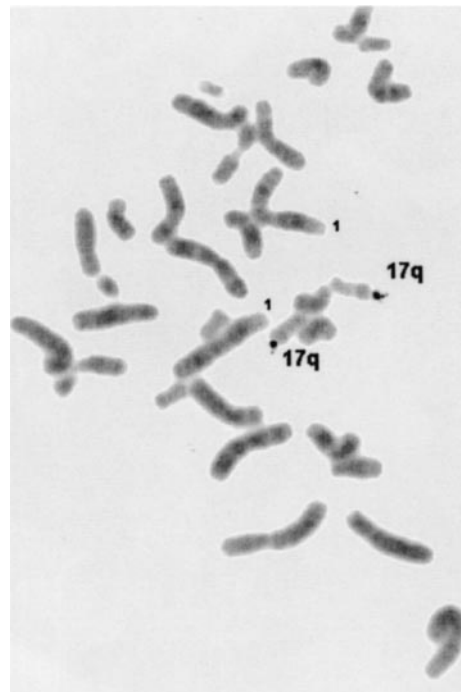


FIG. 2. Localization of the genes encoding FN3K-RP and FN3K to 17qter by FISH.

Two FN3K pseudogene fragments were identified on chromosome 22. One corresponds to exon 2 flanked by parts of introns 1 and 2 and the other to exon 3, intron 3, and exon 4, with adjacent parts of introns 2 and 4. They both share >95% identity with the human FN3K gene, indicating recent duplication events of portions of the FN3K gene.

As Szwergold, Howell, and Beisswenger (17) reported the localization of the FN3K gene on chromosome 1, we checked the chromosomal localization by fluorescence in-situ hybridization (FISH). For this, a PAC clone containing the FN3K gene (no. 127J18) was identified on human RPCI-1 PAC filters (28) by hybridization of a human FN3K probe. PCR amplification of introns using exonic primers showed that this clone contained both FN3K and FN3K-RP genes (not shown). FISH analysis indicated that it hybridized with the telomeric region of chromosome 17 (Fig. 2). No signal was detected on chromosome 1.

**Tissue distribution of FN3K and FN3K-RP.** Northern blots (Fig. 3) showed that the mouse FN3K mRNA is about 1.1 kb in length, which is in agreement with the published sequence (16), whereas the FN3K-RP mRNA is much longer, indicating the presence of an ~2 kb 3' untranslated region. Both mRNAs show the highest levels of expression in bone marrow, brain, spleen, kidney, and lens (allowing for the lower amount of RNA loaded onto the gels in the latter case). Specific expression of FN3K-RP was also observed in testis, thymus, and lungs. Both FN3K and FN3K-RP are also expressed at lower levels in heart, liver, and skeletal muscle. No expression was observed in the intestinal mucosa.

**Overexpression and partial purification of FN3K-RP.** Attempts were made to express both human and mouse FN3K-RPs in *E. coli* using pET3a as a vector and *E. coli* BL21pLysS as host cells. In the case of mouse FN3K-RP, SDS-PAGE analysis indicated that an insoluble protein



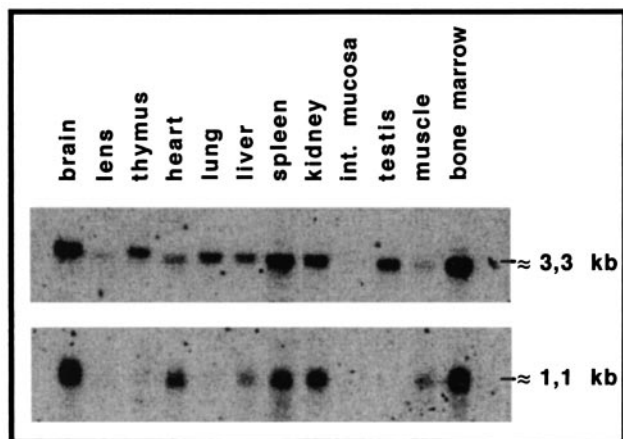


FIG. 3. Tissue distribution of the mRNAs encoding FN3K and FN3K-RP. Total RNA from the indicated tissues (25  $\mu$ g for all tissues except lens, for which  $\sim$ 0.5  $\mu$ g was used) was electrophoresed and hybridized with a probe corresponding to mouse FN3K (lower panel) or mouse FN3K-RP (upper panel).

with the expected mass ( $\sim$ 34 kDa) was obtained. This protein cross-reacted with rabbit polyclonal antibodies raised against human FN3K, with an approximately three-fold lower reactivity than human FN3K (not shown). No expression of human FN3K-RP could be detected.

We therefore resorted to expression in eukaryotic cells. Extracts of HEK cells that had been transfected with plasmids driving the expression of human FN3K or human FN3K-RP were chromatographed on Blue Sepharose, which is known to strongly retain FN3K (16). Proteins were eluted from the column with a salt gradient. Analysis of the fractions by Western blotting with anti-FN3K antibodies indicated the presence of FN3K in the fractions eluted with a high salt concentration from the column loaded with the extracts of cells expressing human FN3K (Fig. 4A). A protein eluting with lower salt concentrations was detected with the same antibodies in the fractions of the column loaded with FN3K-RP (Fig. 4B). None of these proteins could be detected in fractions of a column on which an extract of cells transfected with a control plasmid had been loaded (not shown). These results indicated that soluble FN3K-RP was expressed in HEK cells and that this protein had a distinct chromatographic behavior as compared with FN3K. Coomassie Blue staining of SDS-PAGE gels indicated that this protein accounted for  $\sim$ 10% of total protein in fractions 4 to 6 of the column shown in Fig. 4A.

**Enzymatic activity of FN3K-RP.** As shown in Fig. 4A, overexpressed FN3K catalyzed the phosphorylation of protein-bound fructosamines, whereas no such activity was observed with FN3K-RP. We therefore undertook a more systematic screening of ketosamines as potential substrates of FN3K-RP (and of FN3K) and found that both enzymes catalyzed the phosphorylation of proteins that had been glycosylated with allose and which therefore contained "psicosamines." In the case of FN3K, the kinase activity observed was about 1.6-fold higher with D-allose-glycosylated lysozyme than with glucose-glycosylated lysozyme, but this is presumably due to the higher glycation extent observed in the former than in the latter case (3.3 vs. 1.3 mol/mol). Both proteins were also found to phosphorylate

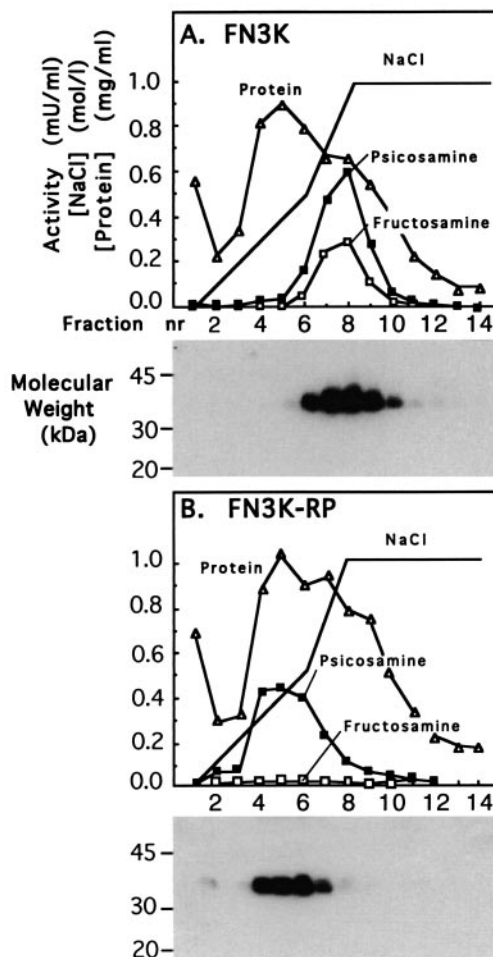


FIG. 4. Partial purification of FN3K (A) and FN3K-RP (B) on Blue Sepharose: coelution of FN3K-RP with a psicosamine kinase activity. Extracts of HEK cells transfected with a plasmid encoding FN3K or FN3K-RP were loaded onto Blue Sepharose columns, which were washed and eluted with the indicated NaCl gradient. Psicosamine kinase (psicosamine,  $\blacksquare$ ) and fructosamine kinase (fructosamine,  $\square$ ) activities were measured using lysozyme glycosylated with allose or glucose as substrates, respectively. The protein concentration ( $\Delta$ ) is also shown. The fractions were analyzed by Western blotting using a polyclonal antibody raised against human recombinant FN3K.

lysozyme that had been glycosylated with D-ribose (results not shown).

These findings prompted us to study the phosphorylation of low-molecular weight psicosamines and ribulosamines. Both FN3K and FN3K-RP were found to phosphorylate 1-deoxy-1-morpholino-psicose, psicoselysine, and 1-deoxy-1-morpholino-ribulose, but only FN3K phosphorylated 1-deoxy-1-morpholino-fructose (Table 1) and fructoselysine (not shown). With both enzymes, the  $K_M$  values for the model ribulosamine were 40- to 80-fold lower than for the low-molecular weight psicosamines, but only about 3- to 4-fold lower than the  $K_M$  for 1-deoxy-1-morpholino-fructose in the case of FN3K. Furthermore, the latter enzyme displayed an  $\sim$ 10-fold higher  $V_{max}$  with 1-deoxy-1-morpholino-fructose than with 1-deoxy-1-morpholino-ribulose.

We also tested the ability of the low-molecular weight ketosamines to inhibit the phosphorylation of lysozyme glycosylated with allose or with ribose. When the substrate was lysozyme glycosylated with allose, FN3K was inhibited

TABLE 1  
Kinetic properties of FN3K and FN3K-RP

	FN3K (ketosamine 3-kinase 1)			FN3K-RP (ketosamine 3-kinase 2)			
	$K_M$ ( $\mu\text{mol/l}$ )	$V_{\text{max}}$ (mU/mg)	$I_{50}$ lys-allose ( $\mu\text{mol/l}$ )	$K_M$ ( $\mu\text{mol/l}$ )	$V_{\text{max}}$ (mU/mg)	$I_{50}$ ( $\mu\text{mol/l}$ )	$I_{50}$ lys-ribose
Deoxymorpholino-fructose	10	46	$67 \pm 22$ ( $n = 3$ )	No substrate	No substrate	No inhibition at 25 mmol/l	No inhibition at 25 mmol/l
Deoxymorpholino-psicose	160	29	690	160	41	$580 \pm 70$ ( $n = 4$ )	$\leq 10\%$ inhibition at 5 mmol/l
Psicoselysine	140	54	$720 \pm 110$ ( $n = 4$ )	$270 \pm 10$ ( $n = 3$ )	$40 \pm 3$ ( $n = 3$ )	480	$\leq 10\%$ inhibition at 5 mmol/l
Deoxymorpholino-ribulose	$2.6 \pm 0.1$ ( $n = 4$ )	5	3.6	$3.5 \pm 0.1$ ( $n = 3$ )	16 ( $n = 3$ )	$6.4 \pm 1.0$ ( $n = 4$ )	$35 \pm 3\%$ inhibition at 100 $\mu\text{mol/l}$

Data are the means of two values or means  $\pm$  SE. For both enzymes, the first two columns indicate the  $K_M$  and  $V_{\text{max}}$  values for the indicated compounds. The third and fourth columns show the concentrations of compounds needed to cause 50% inhibition of the enzymatic activity ( $I_{50}$ ) determined on lysozyme glycosylated with allose or with ribose or the inhibition reached at the indicated concentration. The preparation of enzymes used were purified recombinant human FN3K expressed in *E. coli* (16) and FN3K-RP purified from HEK-293 cells. For the calculation of the  $V_{\text{max}}$ , the concentration of FN3K or FN3K-RP was estimated from SDS-PAGE gels that had been stained with Coomassie Blue by comparison with standards.

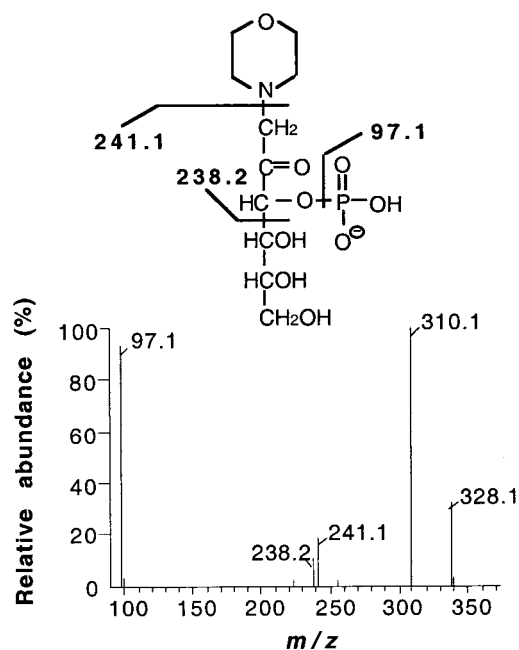


FIG. 5. Tandem mass spectrometry analysis of phosphorylated 1-deoxy-1-morpholino-psicose. The fragmentation spectrum of the deprotonated molecular ion at  $m/z$  328 is shown. The ion at  $m/z$  310 is most likely a dehydration product.

with all four investigated compounds, including 1-deoxy-1-morpholino-fructose, whereas FN3K-RP was inhibited by only the two psicossamines and the ribulosamine without effect of the fructosamine. 1-Deoxy-1-morpholino-tagatose (the C4 epimer of 1-deoxy-1-morpholino-fructose) was a very weak inhibitor of FN3K-RP ( $I_{50} > 5$  mmol/l), whereas it inhibited FN3K with an  $I_{50}$  of 0.25 mmol/l (not shown). 1-Deoxy-1-morpholinoxylulose was much poorer as an inhibitor of FN3K and FN3K-RP ( $I_{50} \sim 350$   $\mu\text{mol/l}$ ) than 1-deoxy-1-morpholino-ribulose, indicating that the effect of the latter was not due to contamination by the C3 epimer (see RESEARCH DESIGN AND METHODS). Both FN3K and FN3K-RP were poorly sensitive to the low-molecular weight psicossamines and ribulosamine when the phosphorylation of lysozyme glycosylated with ribose was investigated, probably due to the high affinity of both enzymes for protein-bound ribulosamines.

**Identification of the phosphorylated carbon.** To determine the identity of the carbon phosphorylated by FN3K-RP, 1-deoxy-1-morpholino-psicose was phosphorylated with this enzyme, purified, and analyzed by tandem mass spectrometry and NMR spectroscopy (Fig. 5). The first technique indicated that the purified product contained a major anion of  $m/z$  328.1, which corresponds to the mass expected for 1-deoxy-1-morpholino-psicose-phosphate. Fragmentation of the latter yielded fragments of  $m/z$  97.1 (corresponding to a phosphate group), 238.2 (corresponding to the loss of C4-C6 of the sugar moiety), and 241.1 (corresponding to the loss of the morpholine moiety). As in the case of 1-deoxy-1-morpholino-fructose 3-phosphate (16), the fact that C4-C6 can be removed without loss of the phosphate group indicates that phosphate is esterified to carbon 3.

Four doublet resonances were detected in the phospho-monoester region of the proton-coupled  $^{31}\text{P}$ -NMR spec-

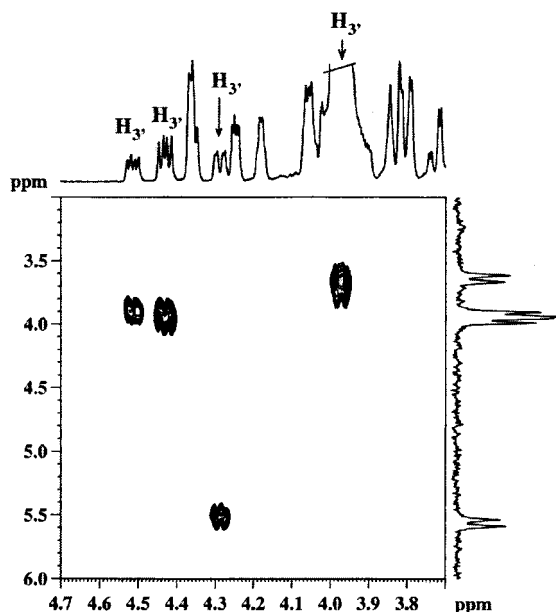


FIG. 6.  $^1\text{H}$ - $^{31}\text{P}$  correlation spectrum through multiple-bond coupling (HMBC) of synthesized 1-deoxy-1-morpholino-psicose-phosphate. Spectra were run on a Bruker DRX500 at a probe head temperature of  $30^\circ\text{C}$ . The pH value of the solution was 6.0. The proton resonances assigned to  $\text{H}_3$  in the four forms of the metabolite are labeled in the proton spectrum. The one-dimensional, proton-coupled  $^{31}\text{P}$  spectrum is also represented.

trum of the sample (ordinate of Fig. 6) and assigned to the four configurational forms of the phosphorylated sugar. The relative abundances were 1:1:1.7:1.2, and the chemical shifts at pH 6.0 were 5.56, 3.97, 3.92, and 3.64 ppm, respectively.  $^1\text{H}$ -NMR spectra with (not shown) and without (abscissa of Fig. 6) phosphorus broadband decoupling, as well as  $^1\text{H}$ - $^{31}\text{P}$ -HMBC spectra (Fig. 6), were acquired to identify the proton resonances that were coupled to phosphorus. In order to determine which proton in the psicose moiety was coupled to phosphorus, proton-proton COSY were acquired. The assignment of protons bound to position 3 followed from the observation that the corresponding resonances correlated only with one other resonance in COSY. This conclusion was corroborated by the observation that the proton multiplets in the  $^1\text{H}$ -spectrum collapsed to doublet resonances when phosphorus decoupling was applied (not shown).

## DISCUSSION

**Enzymatic activity of FN3K-RP and FN3K.** The new enzyme that we describe in the present study phosphorylates psicosaamines and ribulosaamines, though not fructosaamines. The phosphorylated carbon could be identified as C3 by analysis of the phosphorylation product of 1-deoxy-1-morpholino-psicose by both mass spectrometry and NMR spectroscopy. It is most likely that the same carbon is phosphorylated in other substrates, particularly because the homologous enzyme FN3K also phosphorylates the third carbon of the sugar portion of its substrates. FN3K-RP therefore appears to be a ketosamine-3-kinase with a distinct substrate specificity as compared with FN3K.

Another new finding reported in the present article is that FN3K has a much broader substrate specificity than

previously thought because it acts not only on fructosaamines but also on other ketosaamines, with comparable (ribulosaamines) or significantly lower affinities (psicosaamines and maybe also tagatosaamines, which were found to act as inhibitors) than it displays for fructosaamines. This enzyme is therefore also a ketosamine-3-kinase. It is, however, the only enzyme that acts on fructosaamines, which are probably quantitatively the most important ketosaamines that are formed under physiological conditions. Furthermore, it displays a higher catalytic efficiency ( $V_{\text{max}}/K_M$  ratio) on a model fructosamine (1-deoxy-1-morpholino-fructose) than on the equivalent ribulosaamine (1-deoxy-1-morpholino-ribulose). Therefore, its name "fructosamine-3-kinase" appears justified, although its designation as "ketosamine-3-kinase 1" and that of FN3K-RP as "ketosamine-3-kinase 2" would be more rigorous. For the sake of clarity, the names FN3K and FN3K-RP will be used in the rest of the DISCUSSION.

## Chromosomal localization and tissular distribution.

The gene encoding FN3K-RP is located next to the one encoding FN3K in both the human and mouse genomes, indicating an ancestral duplication event. The localization on human chromosome 17, as now reported in databases, was confirmed by in-situ hybridization with a PAC clone containing both genes. The previous localization of the FN3K gene on chromosome 1 (17) is most likely due to uncertain assignment of some PAC clones in an earlier phase of the human genome sequencing project.

Previous RT-PCR experiments performed on human RNAs indicated a widespread tissular distribution of FN3K, with particularly high levels in kidney (17). The Northern blots performed on mouse tissues in the present study indicate a wide variability of expression level from tissue to tissue. The most intense signals were observed with RNA from bone marrow, brain, and kidney, whereas other organs such as liver, intestinal mucosa, testis, thymus, and lung have no or barely detectable mRNA. It is not known at present if this difference in tissular distribution is due to a species difference or to a difference in the technique that was used.

**Physiological function.** Recent work indicates that the function of FN3K is most likely to remove fructosamine residues from proteins (17,18). Fructosamine 3-phosphates are indeed unstable and decompose slowly to 3-deoxyglucosone, inorganic phosphate, and an amine (18). FN3K therefore appears to be a protein-repair enzyme. Such enzymes are expected to play an important role in tissues that contain proteins with long (half-)lives. This is certainly the case of erythrocytes and lenses (29), but it is also true for brain, where myelin proteins have a half-life much longer than 10 days (30). Interestingly, the knockout of another protein-repair enzyme, isoaspartyl-methyl-transferase (31), resulted in intractable seizures, leading to death of the mice after a few weeks. This result underlines the importance of protein-repair mechanisms in the brain and is consistent with the finding of elevated mRNA levels for both FN3K and FN3K-RP in this tissue.

As all ketosamine 3-phosphates other than fructosamine 3-phosphates are most likely also unstable, FN3K-RP could also potentially play the role of a deglycating enzyme. The most puzzling question is that of the identity of the substrates upon which this enzyme is acting physio-



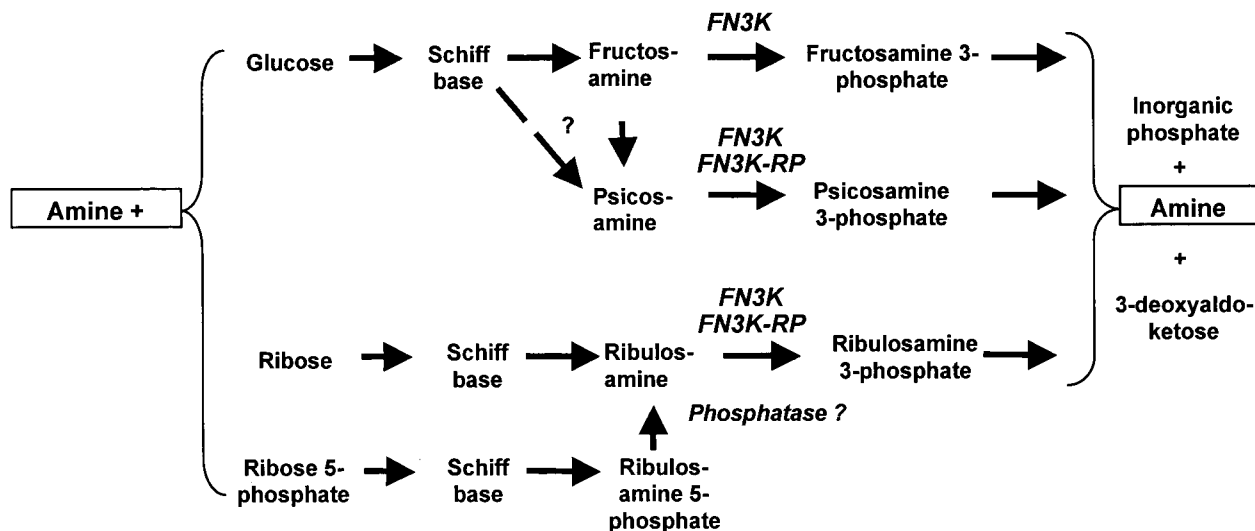


FIG. 7. Reactions catalyzed by FN3K and FN3K-RP and their potential role in the deglycation of proteins. Psicossamines would hypothetically be formed from the Schiff base resulting from the condensation of amines with glucose or through epimerization of fructosamines. Ribulosamines, which can form directly from *D*-ribose, could also hypothetically derive from the enzymatic removal of a phosphate group from ribulosamine 5-phosphates arising from the condensation of an amine with ribose 5-phosphate. Spontaneous breakdown of ketosamine 3-phosphates is known to result in the formation of 3-deoxyglucosone in the case of fructosamine 3-phosphates. The analogous reaction with psicossamine 3-phosphates and ribulosamine 3-phosphates should lead to the formation of 3-deoxyglucosone and 3-deoxypentosone, respectively.

logically. Its best *in vitro* substrates are two compounds with a hydroxyl group in the *D* configuration on C3 (*D*-ribulosamines and *D*-psicossamines), whereas it displays little if any affinity for ketosamines with an *L* configuration in C3. Fructosamines are indeed neither substrates nor inhibitors of FN3K-RP, and a tagatosamine and a xylulosamine were found to be poor inhibitors of this enzyme.

The question then is to know if and how these substrates could arise *in vivo*. As allose is not a physiological sugar, it cannot be a source of psicossamines. These could, however, arise through epimerization of fructosamines or of an intermediate in the formation of Amadori products from glucose (Fig. 7). Preliminary data indicate that when proteins are incubated with elevated concentrations of glucose in the presence of 200 mmol/l inorganic phosphate, which facilitates the formation of fructosamines (32), a substrate of FN3K-RP forms (F.C., E.V.S., unpublished data), suggesting that epimerization around the third carbon of fructosamines takes place under these conditions.

Ribulosamines could hypothetically form either directly through reaction of amines with *D*-ribose or indirectly through reaction with ribose 5-phosphate (Fig. 7) or ADP-ribose, followed by (enzymatic?) removal of phosphate or ADP. Little is known about the concentration of free ribose, ribose 5-phosphate, and ADP-ribose in most cell types. It is, however, worth mentioning that the latter two are extremely powerful glycation agents (7,8) and that it would therefore make sense to have an enzymatic system able to remove the corresponding Amadori products from proteins. As hyperglycemia stimulates the activity of the pentose phosphate pathway (33), poor glycemic control could also favor glycation by ribose 5-phosphate, further linking the new enzyme with diabetes.

Further evidence for a role of the new enzyme in combating glucose-induced glycation is to be found in the observation that the incubation of erythrocytes with an elevated glucose concentration under the conditions pre-

viously described (18) leads to the formation of substrates not only for FN3K but also FN3K-RP (G.D., F.C., J. Fortpied, and E.V.S., unpublished data). The identity of the FN3K-RP substrates formed under these conditions still remains to be determined; psicossamines and ribulosamines are both likely candidates.

Compared with FN3K-RP, FN3K has the unique capacity to phosphorylate fructosamines, suggesting that one of its important functions is to repair damages provoked by glucose. As both ketosamine-3-kinases phosphorylate psicossamines and ribulosamines with similar affinities, one may wonder if FN3K-RP has any specific role to play. One possibility is that this enzyme is able to phosphorylate as yet unknown substrates that are not utilizable by FN3K. In addition, it should be stressed that FN3K-RP appears to be expressed in tissues (testis and lung) where the FN3K mRNA is undetectable. In conclusion, the data reported in the present article indicate the existence of an enzyme that may complement the action of FN3K in a putative deglycation process.

#### ACKNOWLEDGMENTS

This work was supported by the Concerted Research Action Program of the Communauté Française de Belgique; the Belgian Federal Service for Scientific, Technical, and Cultural Affairs; the European Foundation for the Study of Diabetes; and a grant from the European Community (Euroglycan network, QLG1-CT-2000-00047). F.C. is a fellow of the Fonds pour l'Encouragement à la Recherche dans l'Industrie et dans l'Agriculture, and G.D. is a Chargé de Recherche of the Belgian Fonds National de la Recherche Scientifique.

The authors thank Geneviève Berghenouse for her help in experimental work, Helena Santos (Lisbon) for running and interpreting the NMR spectra, Didier Vertommen for his help in mass spectrometry analysis, and Maria Veiga-da-Cunha for her thoughtful comments.

GenBank accession nos.: AY360465, human fructosamine-3-kinase-related protein (human FN3K-RP); AY360466, mouse fructosamine-3-kinase-related protein (mouse FN3K-RP).

## REFERENCES

- Hodge JE: The Amadori rearrangement. *Adv Carbohydr Chem* 10:169–205, 1955
- Baynes JW, Watkins NG, Fisher CI, Hull CJ, Patrick JS, Ahmed MU, Dunn JA, Thorpe SR: The Amadori product on protein: structure and reactions. *Prog Clin Biol Res* 304:43–67, 1989
- Yaylayan VA, Huyghues-Despointes A: Chemistry of Amadori rearrangement products: analysis, synthesis, kinetics, reactions, and spectroscopic properties. *Crit Rev Food Sci Nutr* 34:321–369, 1994
- Heyns K, Meynecke KH: Über Bildung und Darstellung von D-Glukosamin aus Fruktose und Ammoniak. *Chem Ber* 86:1453–1462, 1953
- Bunn HF, Higgins PJ: Reaction of monosaccharides with proteins: possible evolutionary significance. *Science* 213:222–224, 1981
- Haney DN, Bunn HF: Glycosylation of hemoglobin in vitro: affinity labeling of hemoglobin by glucose-6-phosphate. *Proc Natl Acad Sci U S A* 73:3534–3538, 1976
- Kun E, Chang AC, Sharma ML, Ferro AM, Nitecki D: Covalent modification of proteins by metabolites of NAD<sup>+</sup>. *Proc Natl Acad Sci U S A* 73:3131–3135, 1976
- Jacobson EL, Cervantes-Laurean D, Jacobson MK: ADP-ribose in glycation and glycoxidation reactions. *Adv Exp Med Biol* 419:371–379, 1997
- Goldstein DE, Little RR, Wiedmayer HM, England JD, McKenzie EM: Glycated hemoglobin: methodologies and clinical applications. *Clin Chem* 32:B64–70, 1986
- Johnson RN, Metcalf PA, Baker JR: Fructosamine: a new approach to the estimation of serum glycosylprotein: an index of diabetic control. *Clin Chem Acta* 127:87–95, 1982
- Armbruster DA: Fructosamine: structure, analysis and clinical usefulness. *Clin Chem* 33:2153–2163, 1987
- Cohen MP, Clements RS, Cohen JA, Shearman CW: Glycated albumin promotes a generalized vasculopathy in the db/db mouse. *Biochem Biophys Res Commun* 218:72–75, 1996
- Baynes JW: Role of oxidative stress in development of complications in diabetes. *Diabetes* 40:405–412, 1991
- Vlassara H, Bucala R, Striker L: Pathogenic effects of advanced glycosylation: biochemical, biologic, and clinical implications for diabetes and aging. *Lab Invest* 70:138–151, 1994
- Brownlee M: Biochemistry and molecular cell biology of diabetic complications. *Nature* 414:813–820, 2001
- Delpierre G, Rider MH, Collard F, Stroobant V, Vanstapel F, Santos H, Van Schaftingen E: Identification, cloning, and heterologous expression of a mammalian fructosamine-3-kinase. *Diabetes* 49:1627–1634, 2000
- Szwergold BS, Howell S, Beisswenger PJ: Human fructosamine-3-kinase: purification, sequencing, substrate specificity, and evidence of activity in vivo. *Diabetes* 50:2139–2147, 2001
- Delpierre G, Collard F, Fortpied J, Van Schaftingen E: Fructosamine-3-kinase is involved in an intracellular deglycation pathway. *Biochem J* 365:801–808, 2002
- Finot PA, Bricout J, Viani R, Mauron J: Identification of a new lysine derivative obtained upon acid hydrolysis of heated milk. *Experientia* 24:1097–1099, 1968
- Hodge JE, Rist CE: The Amadori rearrangement under new conditions and its significance for non-enzymatic browning reactions. *J Am Soc* 75:316–322, 1953
- Park JT, Johnson MJ: A submicrodetermination of glucose. *J Biol Chem* 181:149–151, 1949
- Kozak M: An analysis of 5'-noncoding sequences from 699 vertebrate messenger RNAs. *Nucleic Acid Res* 20:8125–8132, 1987
- Alessi DR, Cohen P: Mechanism of activation and function of protein kinase B. *Curr Opin Genet Dev* 8:55–62, 1998
- Bradford MM: A rapid and sensitive method for the quantification of microgram quantities of protein utilizing the principle of protein-dye binding. *Anal Biochem* 72:248–254, 1976
- Sambrook J, Fritsch EF, Maniatis T: *Molecular Cloning: A Laboratory Manual*. 2nd ed. Cold Spring Harbor, NY, Cold Spring Harbor Laboratory Press, 1989
- Delpierre G, Vanstapel F, Stroobant V, Van Schaftingen E: Conversion of a synthetic fructosamine into its 3-phospho derivative in human erythrocytes. *Biochem J* 352:835–839, 2000
- Persson B, Flinta C, von Heijne G, Jörnvall H: Structures of N-terminally acetylated proteins. *Eur J Biochem* 152:523–527, 1985
- Ioannou PA, de Jong PJ: Construction of bacterial artificial chromosome libraries using the modified P1 (PAC) system. In *Current Protocols in Human Genetics*. Dracopoli et al., Eds. New York, Wiley, 1996
- Delcour J, Papaconstantinou J: Biochemistry of bovine lens proteins. IV: synthesis and aggregation of alpha-crystallin subunits in differentiating lens cells. *J Biol Chem* 247:3289–3295, 1972
- Lajtha A, Toth J, Fujimoto K, Agrawal HC: Turnover of myelin proteins in mouse brain in vivo. *Biochem J* 164:323–329, 1977
- Kim E, Lowenson JD, MacLaren DC, Clarke S, Young SG: Deficiency of a protein-repair enzyme results in the accumulation of altered proteins, retardation of growth, and fatal seizures in mice. *Proc Natl Acad Sci U S A* 94:6132–6137, 1997
- Watkins NG, Neglia-Fisher CI, Dyer DG, Thorpe SR, Baynes JW: Effect of phosphate on the kinetics and specificity of glycation of protein. *J Biol Chem* 262:7207–7212, 1987
- Keogh RJ, Dunlop ME, Larkins RG: Effect of inhibition of aldose reductase on glucose flux, diacylglycerol formation, protein kinase C, and phospholipase A2 activation. *Metabolism* 46:41–47, 1997